Available online at www.sciencedirect.com
SCIENCE DIRECT®
Nuclear Instruments and Methods in Physics Research A 497 (2003) 294–304
NUCLEAR INSTRUMENTS & METHODS IN PHYSICS RESEARCH Section A
www.elsevier.com/locate/nima

Radiation hardness and lifetime studies of the VCSELs for the ATLAS SemiConductor Tracker

P.K. Teng[a], T. Weidberg[b,*], M.L. Chu[a], T.S. Duh[c], I.M. Gregor[d,1], L.S. Hou[a], S.-C. Lee[a], P.S. Song[c], D.S. Su[a]

[a] *Institute of Physics, Academia Sinica, Taiwan*
[b] *Physics Department, Oxford University, UK*
[c] *Institute of Nuclear Energy Research, Taiwan*
[d] *Wuppertal University, Germany*

Received 17 June 2002; received in revised form 25 September 2002; accepted 10 October 2002

Abstract

Studies have been performed on the radiation hardness of the type of VCSELs[2] that will be used in the ATLAS SemicConductor Tracker. The measurements were made using 30 MeV proton beams, 24 GeV/c proton beams and a gamma source. The lifetime of the devices after irradiation was studied.

Keywords: LHC; Data transmission; Optoelectronics; VCSELs; Radiation tolerance

1. Introduction

Optical links will be used in the ATLAS SemiConductor Tracker (SCT) [1] to transmit data from the silicon strip detector modules to the off-detector electronics and to distribute the Timing, Trigger and Control (TTC) data from the counting room to the front-end electronics [2]. There will be 8176 VCSELs inside the SCT. During the operation of the SCT at the Large Hadron Collider (LHC), all the on-detector components will be exposed to large fluences of charged and neutral particles. The SCT on-detector components have been designed to be sufficiently radiation tolerant to survive 10 years of LHC operation. The results of the radiation hardness studies of the ASICs, epitaxial silicon PIN photodiodes and fibres are described in previous publications [3–8]. This paper presents the results of radiation hardness tests on the type of VCSELs to be used in the SCT. Previous publications have shown that other types of VCSELs are sufficiently radiation hard for use in ATLAS [6,9].

An overview of the radiation damage and reliability theory is given in Section 2. The expected radiation environment is defined in Section 3. The experimental set-up and radiation

*Corresponding author. Department of Particle and Nuclear Physics, Nuclear Physics Laboratory, Keble Road, Oxford OX1 3RH, UK. Tel.: +44-1865-273370; fax: +44-1865-273418.
E-mail address: t.weidberg@physics.oxford.ac.uk (T. Weidberg).
[1] Now at DESY, Zeuthen, Germany.
[2] Vertical Cavity Surface Emitting Lasers.

0168-9002/03/$ - see front matter
PII: S0168-9002(02)01922-8

sources used are described in Section 4. The results of the radiation hardness studies are discussed in Section 5. The accelerated ageing tests are described in Section 6 and finally some conclusions are drawn in Section 7.

2. Radiation damage and reliability theory for VCSELs

2.1. Radiation damage theory

The main effect of radiation on the GaAlAs VCSELs is expected to be due to displacement damage. The interaction of high-energy particles with atoms in the semiconductor lattice may cause an atom to be dislodged from its position in the lattice. The primary knock atom (PKA) may create a cascade of collisions which can induce large complexes of point defects in the crystal structure. Some of these defects are stable and can create new energy levels in the semiconductor band-gap. Therefore, these defects in the crystal structure can act as non-radiative recombination centres, which decreases the minority carrier lifetime. For LEDs this will cause a decrease in the light output if the non-radiative decay rate is similar to or larger than the radiative decay rate. For semiconductor lasers such as VCSELs, the minority carrier lifetime in the lasing regime is dominated by stimulated emission and is therefore very short. However below the laser threshold, the lifetime is determined by spontaneous emission as in LEDs. Therefore the main effect of radiation damage for VCSELs is expected to be an increase in the threshold current.

In previous studies, significant amounts of annealing of the radiation damage in VCSELs were observed when the devices were operated under forward bias (injection annealing) [6,9,10]. The effects of annealing with forward currents of 10 and 20 mA were studied in this work.

2.2. Reliability theory

The lifetime of semiconductor lasers such as VCSELs can be limited by effects such as impurity diffusion, electro-migration and inter-metalic component formation. These processes can create so called Dark Line Defects (DLDs) which appear as dark lines over the active region of the laser. The rate of formation of these defects and hence the lifetime of the devices have been found to have an exponential change with temperature. The lifetime also depends on the current density and hence on the operating current. An empirical relationship, the Arrhenius equation has been found to give a good fit to VCSEL reliability data. The Arrhenius equation

$$\mathrm{AF} = \left(\frac{I_2}{I_1}\right)^2 \exp\left\{\frac{E_A}{k_B}\left(\frac{1}{T_1} - \frac{1}{T_2}\right)\right\} \tag{1.1}$$

predicts the acceleration factor for ageing when comparing operating conditions with different temperatures (T_1 and T_2) and operating currents (I_1 and I_2). The current factor is required to account for the effect of operating current on reliability over and above its effect on junction temperature [11]. The data from the study presented in Ref. [11] shows a good agreement with the factor of the square of the operating current in Eq. (1.1). E_A is the activation energy and is commonly assumed to be 1.0 eV [12]. The acceleration factor AF gives the ratio between the mean time to failure at the two different operating conditions. Accelerated ageing studies of unirradiated VCSELs by different manufacturers show good agreement with the Arrhenius equation [11,13,14]. The data from the manufacturer's of the VCSELs used in this study, gave results which were consistent with an activation energy of 1.0 eV [14].

Due to the great improvements in process control, the lifetimes of the current generation of VCSELs are very large and the reliability would be expected to be considerably better than that required for 10 yr of LHC operation. The main aim of the lifetime studies presented in this paper is to see if there is any evidence for a large decrease in lifetime after irradiation.

3. Expected radiation environment

The expected radiation environment in the SCT is mainly due to a mixture of high-energy charged particles, low-energy neutrons and photons. The effects of displacement damage in semiconductor

devices have been found to scale with the total non-ionising energy loss (NIEL). There is evidence for NIEL scaling in GaAs electronic devices [15,16], particle detectors [17], as well as GaAlAs LEDs [6]. A further test of the NIEL hypothesis for GaAlAs VCSELs is performed in this work.

The expected spectra of charged and neutral particles in the ATLAS Inner Detector were simulated using the FLUKA transport code. The standard ATLAS luminosity scenario of 3 yr of low luminosity ($10^{33}\,cm^{-2}\,s^{-1}$) followed by 7 yr of high luminosity ($10^{34}\,cm^{-2}\,s^{-1}$) operation was assumed. A safety factor of 1.5 was applied to take into account all the uncertainties in the calculations [1]. It is convenient to convert the fluences into the equivalent fluence of 1 MeV neutrons, assuming the NIEL scaling hypothesis. This is done by integrating the differential spectrum weighted by the ratio of NIEL for a particle of energy E and a 1 MeV neutron.

$$F_{\mathrm{neq}} = \int \frac{\mathrm{d}N}{\mathrm{d}E}\frac{\mathrm{NIEL}(E)}{\mathrm{NIEL}(n_{1\ \mathrm{MeV}})}\mathrm{d}E. \qquad (1.2)$$

The NIEL values for GaAs[3] used were taken from Refs. [16,17]. The resulting fluence for the inner layer of the SCT, which will receive the highest fluence are given in Table 1 below for different particle types and energies.

The expected ionising radiation dose for the inner layer of the SCT during the 10 yr of ATLAS operation is 100 kGy(Si) [1].

Table 1
Expected NIEL values for GaAs and fluences for the inner SCT layer for 10 yr of LHC operation

Particle type	Energy (MeV)	NIEL ($keV\,cm^{-2}\,g^{-1}$)	Fluence ($10^{14}\,cm^{-2}$)
n	1	0.55	9.9
p	30	4.0	1.4
p	24 000	2.9	1.9

4. Experimental set-up and irradiation facilities

4.1. 30 MeV protons

Beams of protons of kinetic energy of 30 MeV were used from the TR-30 Cyclotron Facility of the Institute of Nuclear Energy Research (INER) in Taiwan. The beam currents used were about 10 nA. An external beam line was used and the beam was collimated and allowed to pass through a thin window. The beam spot size is 1 cm in radius at the exit window. The target was placed about 20 cm downstream and the typical flux was about $2\times10^{10}\,cm^{-2}\,s^{-1}$. A photograph of the target and beam line is shown in Fig. 1.

4.1.1. Fluence measurements

A Faraday cup was placed behind the target to collect the charge. The current signal was sent to a digital current integrator[4] and the resulting digital signal was then counted[5]. The total fluence accumulated was $2\times10^{14}\ p\,cm^{-2}$. Assuming the NIEL scaling hypothesis, this is a factor of 40% larger than for the worst case for 10 yr of SCT operation at LHC.

4.1.2. VCSEL power measurements

The VCSELs[6] were wire bonded to carrier PCBs. Five VCSELs were mounted on one carrier PCB but only one VCSEL was powered at a time whilst the power was being measured. The optical power of the VCSELs was measured as a function of the drive current using a large area germanium photodiode as shown in Fig. 2. For each current setting, 10 measurements were taken and the average was given to reduce the error. These power measurements were made before and after the irradiation. The VCSELs were operated at 10 mA current during the irradiation.

4.2. 24 GeV protons

The irradiation was performed at the T7 beam of the CERN Proton Synchrotron (PS) [18]. This is

[3] The active (light emitting) part of a VCSEL is the Multi Quantum Well (MQW) structure. The Trulelight VCSELs used in this study contain three GaAs quantum wells separated by AlGaAs barriers.

[4] ORTEC Model 439.

[5] ORTEC Model 871 Timer and Counter.

[6] Truelight, Taiwan, TSD-8A12.

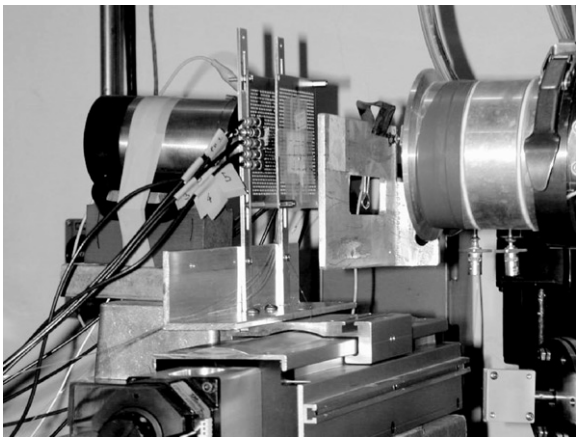

Fig. 1. Faraday cup and VCSELs in the external proton beam line.

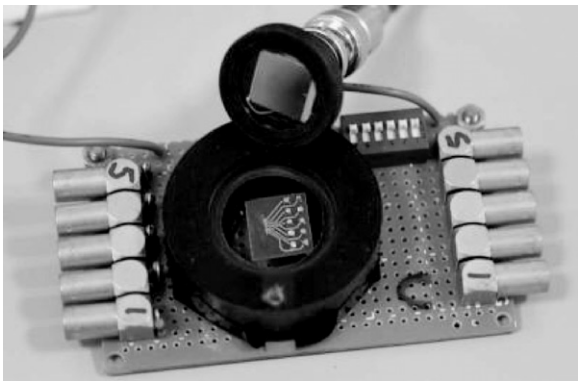

Fig. 2. Photograph showing 5 VCSELs on a carrier board and the large area photodiode used to measure the optical power.

a primary proton beam of momentum 24 GeV/c. There were 3 proton spills per PS supercycle (14.4 s) and the intensity in each spill was $\sim 2 \times 10^{11}$ protons. The beam area was $\sim 4\,cm^2$.

4.2.1. Fluence measurements

The fluence was monitored by secondary emission counters, which were cross-calibrated with aluminium foil activation analysis. The typical proton flux was $\sim 10^{10}\,cm^{-2}\,s^{-1}$ The total proton fluence was $1.09 \times 10^{15}\,cm^{-2}$ and measurements were made after several steps in the fluence.

4.2.2. VCSEL packaging and optical power measurements

The same type of VCSELs was used as for the 30 MeV proton irradiation data (Section 5.1). The VCSELs were packaged in a fibre pig-tailed opto-package. The light from the VCSELs is coupled into the fibres by a reflection from the 45° angle polished fibre. A schematic diagram of the opto-package showing the 8 fibres coupled to 8 VCSELs is shown in Fig. 3. This packaging uses the same technique that will be used for the readout of the ATLAS Barrel SCT detector [19]. These opto-packages used radiation-hard SIMM[7] fibre [8].

They were coupled with ST couplers to a radiation tolerant GRIN[8] fibre [8]. The GRIN fibre was taken out of the radiation zone to an optical power meter. The VCSELs were biased at 10 mA during the irradiation except for short periods when the optical power was measured as a function of the drive current (LI curves). The optical power was measured with a power meter and corrected for the losses in the ST coupler and the GRIN fibre[9]. Only 4 out of 8 VCSELs had sufficiently long lengths of radiation hard fibre for the GRIN fibres to avoid radiation damage; therefore, only these 4 VCSELs are used in this study. For the 4 VCSELs used in the study, the radiation damage induced attenuation in the GRIN fibre was negligible. The radiation damage in the 1 m length of the radiation hard fibre is also expected to be negligible [8].

4.3. Gamma source

The gamma source used was the Mega Curie ^{60}Co Irradiation Plant of the Institute of Nuclear Energy Research (INER), Taiwan. This consists of a plane array of ^{60}Co sources covering an area of

[7] Step Index Multi Mode, S.50/60/125/250 Fujikura, Japan.

[8] Graded Index Multi Mode, Fibre 407E, Plasma Optical Fibre B.V., The Netherlands.

[9] The insertion loss of the ST coupler and patch fibre was determined by the following procedure: a fibre coupled VCSEL was connected to a fibre coupled photodiode (PD) and the current was measured. Then the extra length of patch fibre and ST connector was inserted and the PD current measured. The induced attenuation was then estimated from the ratio of the PD currents.

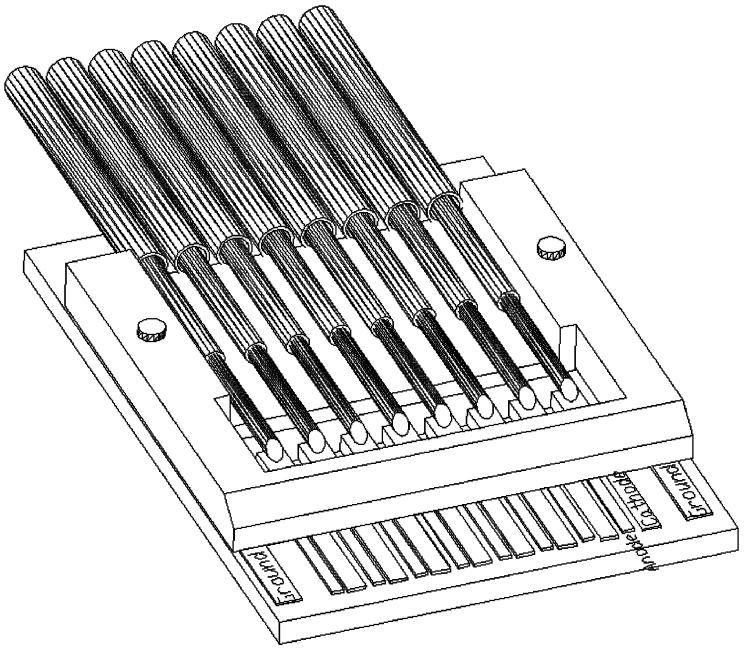

Fig. 3. Schematic diagram of the opto-package containing 8 VCSELs coupled to radiation hard fibre.

approximately $0.2 \times 2\,m^2$. The dose rates used were 60 and 7 kGy(Si)/h. The dosimetry was performed using radiochrome film. The dosimetry was calibrated to be accurate to within 4% by comparisons with measurements at NIST[10] and NPL[11]. The total dose accumulated was 580 kGy(Si) for one group and 600 kGy(Si) for the remaining groups. This is a factor of 6 times higher than that expected during ATLAS operation. The VCSELs were mounted on the same type of carriers as used for the 30 MeV proton irradiation (Section 4.1.2). The optical power of the VCSELs were measured with the same system as that used for the 30 MeV proton irradiation data (Section 4.1.2).

5. Radiation hardness results

The results for the proton and the gamma radiation tests are given below.

[10] National Institute of Standards and Testing, USA.
[11] National Physical Laboratory, London, UK.

5.1. 30 MeV proton tests

A sample of 20 VCSELs was used for these studies. The light output versus forward current (LI curve) for the VCSELs was measured before irradiation and after irradiation and after one week annealing at a constant current of 10 mA. The VCSELs were biased with a current of 10 mA during irradiation. The total time taken for the irradiation was about 3 h so that only a limited amount of annealing would be expected to occur in this period. The results for the first 2 VCSELs in the sample are shown in Figs. 4 and 5.

The LI curves show that there is the expected increase in threshold current with radiation and that there is also a decrease in the slope efficiency. The data taken after one week annealing at 10 mA show a very significant recovery. There is an even greater degree of recovery after one week of annealing at 20 mA. In order to present the data in a more convenient form, a linear fit was made to each VCSEL LI curve, before radiation, after irradiation, after one week annealing at 10 mA and one further week annealing at 20 mA. The fits were

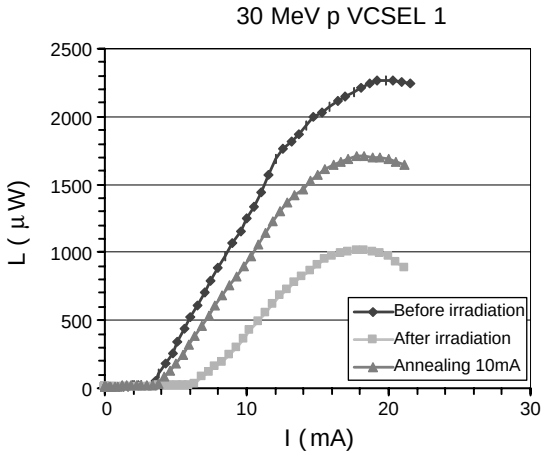

Fig. 4. Optical power versus VCSEL current (LI curves) for the first VCSEL, before irradiation, immediately after irradiation and after one week of annealing at 10 mA.

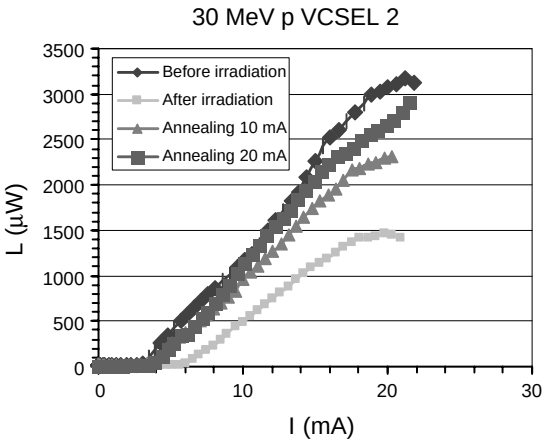

Fig. 5. LI curve for the second VCSEL, before irradiation, immediately after irradiation and after one week of annealing at 10 mA and one further week of annealing at 20 mA.

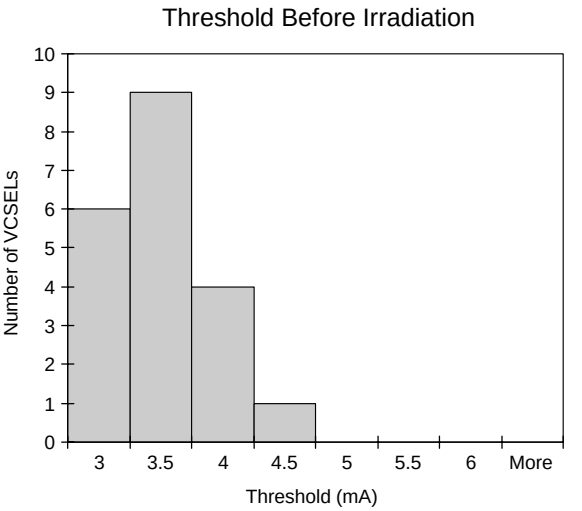

Fig. 6. Distribution of laser thresholds for the sample of VCSELs before irradiation.

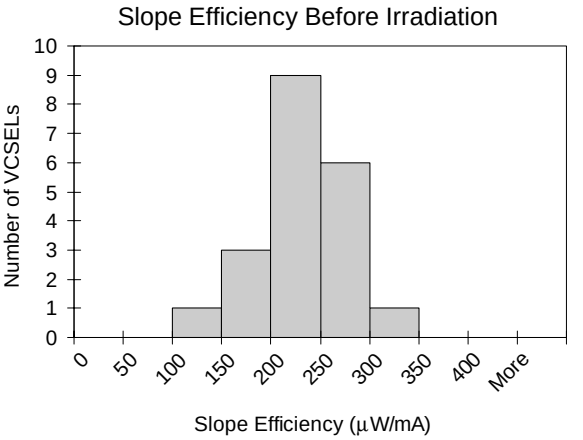

Fig. 7. Distribution of slope efficiencies for the sample of VCSELs before irradiation.

made in the region of light output above 100 μW to the end of the approximately linear regime. The systematic uncertainty due to the choice of fit range was estimated to be ~1%. The fit results gave values for the threshold current and the slope efficiency. The distribution of the fitted values for thresholds and slope efficiencies are shown in Figs. 6 and 7.

The distribution of the increase in laser thresholds immediately after irradiation and after one week of annealing at 10 mA is shown in Figs. 8 and 9. The one VCSEL with an entry in the overflow bin in Fig. 8 had a threshold of 8.2 mA, which however reduced to 2.2 mA after one week of annealing at 10 mA.

The slope efficiencies were calculated for all the VCSELs after irradiation and after one week of annealing at 10 mA. The distribution of the ratio of slope efficiency after irradiation compared to pre-irradiation is shown in Fig. 10 below. The

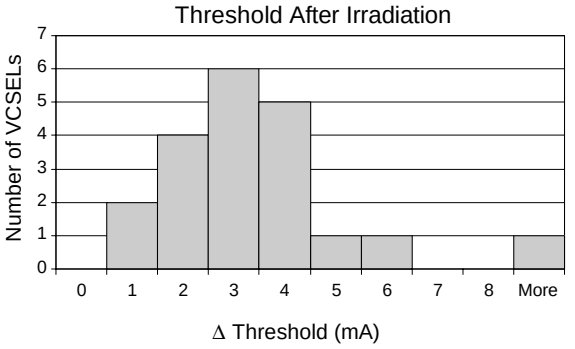

Fig. 8. Distribution of the increase in laser threshold after irradiation compared to before irradiation.

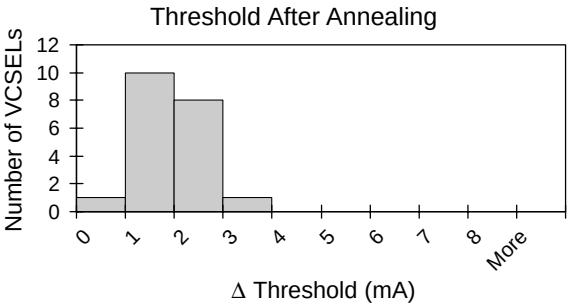

Fig. 9. Distribution of the increase in laser threshold after irradiation and one week of annealing at 10 mA, compared to before irradiation.

equivalent distribution after one week of annealing at 10 mA is shown in Fig. 11.

The mean values of the fitted thresholds and slope efficiencies before and after irradiation and after one week annealing at 10 mA and one further week at 20 mA are summarised in Table 2.

5.2. 24 GeV proton data

The LI curves before irradiation and after several stages of irradiation for one of the 4 VCSELs are shown in Fig. 12.

In order to compare the results from the 24 GeV/c proton irradiation with the 30 MeV proton data, a summary of the results for the 4 VCSEL before irradiation and after a fluence of 1.5×10^{15} $n_{eq}\,cm^{-2}$ are given in Table 3 below. According to the NIEL hypothesis and the NIEL values in Table 1, this fluence should give an equivalent damage to that from the 30 MeV proton irradiation.

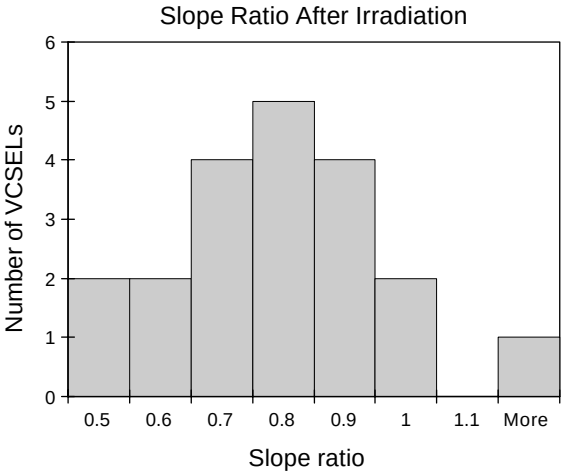

Fig. 10. Distribution of the ratio of slope efficiencies after irradiation compared to before irradiation.

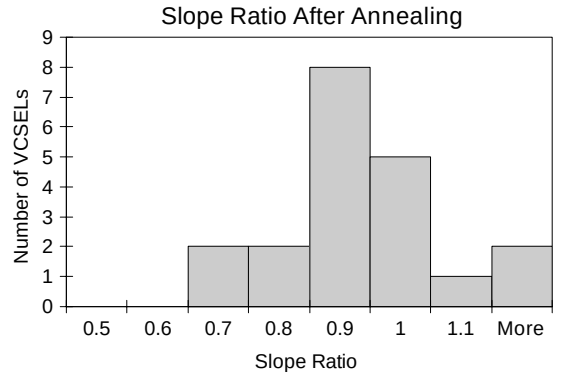

Fig. 11. Distribution of the ratio of slope efficiencies after irradiation and one week of annealing at 10 mA, compared to before irradiation.

5.3. Comparison of 30 MeV and 24 GeV proton data

The threshold before irradiation for this sample of VCSELs irradiated with 24 GeV/c protons is similar to that of the sample used for the 30 MeV

Table 2
Summary of pre- and post-irradiation thresholds and slope efficiencies for the sample of 20 VCSELs irradiated with 30 MeV protons

Parameter	Mean value	Units
Threshold before irradiation.	3.28±0.09	mA
Slope efficiency before irradiation.	180.5±9.8	μW/mA
Increase in threshold current after irradiation.	3.0±0.4	mA
Ratio of slope efficiency after irradiation to before.	0.73±0.04	—
Increase in threshold current after irradiation and one week of annealing at 10 mA compared to before irradiation.	0.94±0.11	mA
Ratio of slope efficiency after irradiation and one week of annealing at 10 mA to before irradiation.	0.88±0.03	—
Increase in threshold current after irradiation and one week of annealing at 10 mA and one week at 20 mA compared to before irradiation.	0.42±0.13	mA
Ratio of slope efficiency after irradiation and one week of annealing at 10 mA and one week at 20 mA to before irradiation.	0.98±0.03	

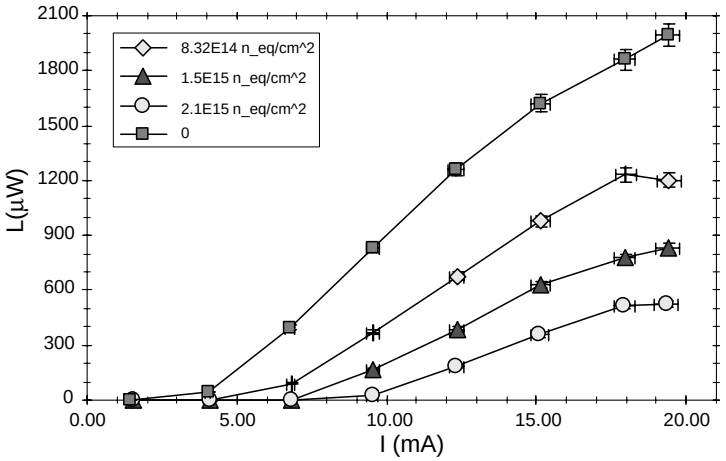

Fig. 12. LI curves for an unirradiated and irradiated VCSEL. The measured proton fluences have been converted to 1 MeV neutron equivalent values using the NIEL values in Table. 1.

Table 3
Summary of before and after irradiation data for the 4 VCSELs in the 24 GeV/c proton irradiation

Parameter	Mean value	Units
Threshold before irradiation	4.33±0.27	mA
Slope efficiency before irradiation	147±23	μW/mA
Increase in threshold current after irradiation	3.74±0.15	mA
Ratio of slope efficiency after irradiation to before	0.60±0.07	—

proton irradiation. The slope efficiency before irradiation is significantly lower in this sample because these devices were coupled to 50 μm core fibres using angle polished fibres; therefore, the coupling is not fully efficient.

The mean increase in threshold and the decrease in slope efficiency are similar but slightly larger than those measured during the 30 MeV proton irradiation. The time taken to reach the same equivalent fluence was about a factor of 3 less for the 30 MeV proton data than for the 24 GeV/c

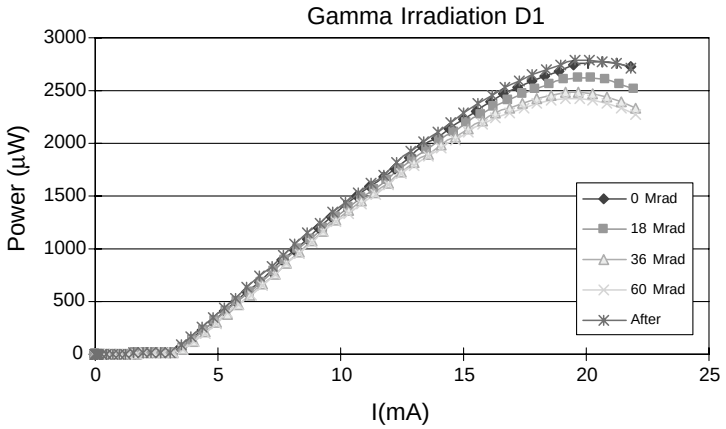

Fig. 13. LI curve of one VCSEL after gamma irradiation to various doses.

proton data. Therefore, this effect cannot explain the difference in the results between the 30 MeV and 24 GeV/c proton data. One would expect slightly more annealing in the 24 GeV/c proton data than in the 30 MeV proton data. The apparent significance of the difference for the threshold shift and the ratio of slope efficiency would be 2.6σ and 1.6σ, respectively. However the statistical significance of these discrepancies cannot be estimated assuming Gaussian statistics because of the very small number of devices in the 30 MeV proton irradiation sample (4 VCSELs).

The probability that larger discrepancies than those observed occurs for two measurements due to statistical fluctuations with the actual sample sizes used was evaluated using a simple "toy" Monte Carlo programme. This programme generated 10 000 samples of the same size as used for the two data sets (20 VCSELs for the 30 MeV proton data and 4 VCSELs for the 24 GeV/c proton data) using pseudo random numbers generated from identical Gaussian distributions. The probability of obtaining a larger difference (in terms of number of σ) between the two data sets for the threshold shift (ratio of slope efficiencies) is 4.3% (17%).

One can therefore conclude that the radiation damage data for 30 MeV protons and for 24 GeV/c protons are consistent within errors with the NIEL scaling hypothesis.

Table 4
Relative light output (RLO) at 10 mA, after irradiation compared to before irradiation

VCSEL set	Biased during irradiation	Dose rate (kGy/h)	Dose (kGy)	Mean RLO
A	No	60	580	0.96 ± 0.03
B	No	7	600	0.98 ± 0.03
C	Yes	60	600	0.95 ± 0.03
D	Yes	60	600	0.96 ± 0.03

5.4. Gamma irradiation results

Two sets of PCBs (sets A and B) each containing 5 VCSELs were placed at two different locations to study any possible dose rate effects. The dose rate was 60 kGy(Si)/h for set A and 7 kGy(Si)/h for set B. The LI curve of the first VCSEL in set A is shown for various doses (Fig. 13).

There is a small decrease in optical power at high current with dose but this is probably due to an increase in temperature during the measurement. Two further sets of 5 VCSELs (sets C and D) were then irradiated under a constant bias current of 10 mA at a dose rate of 60 kGy(Si). The average relative light output at 10 mA after irradiation compared to before irradiation was calculated for each of the 4 sets and the results are given in Table 4.

From these results it can be seen that there is no significant decrease in light output with the gamma

irradiation, even for a dose of a factor of 6 larger than expected for the 10 yr of SCT operation.

6. Lifetime studies

The sample of VCSELs irradiated with 30 MeV protons and subsequently annealed was used for the accelerated ageing studies. 20 VCSELs were operated at a bias current of 10 mA at a temperature of 100°C. The ageing test was operated for a total of 2534 h and no device showed any significant decrease in light output during the tests. It is conventional to define a laser failure as a decrease in light output of more than 3 dB. With this definition there were no failures. This result can be converted into an upper limit on the failure rate using Poisson statistics.

$$R_{\text{fail}} = \left(\frac{1}{N\Delta t}\right)\ln\left(\frac{1}{1-C}\right) \tag{1.3}$$

where N is the total number of devices, Δt is the total time, and C is the confidence level (c.l.) used. At 90% c.l. the failure rate is therefore less than $4.5\times10^{-5}\,\text{h}^{-1}$. This upper limit on the failure rate can be scaled to different temperatures using the Arrhenius equation (1.1). Since the VCSEL ageing is only expected when the devices are powered, other factors are required in order to convert the result to 10 yr of ATLAS operation. A factor of 3 is used to allow for the fraction of a year in which ATLAS will be operating, a factor of two to allow for an equal number of "1s" and "0s" in the data (the SCT data links use NRZ[12] data, therefore no light is used when sending "0s") and a further factor of two to allow for the expected fraction of the time that the data links are sending data. With these assumptions, the expected VCSEL failure rates for different assumed operating temperatures are given in Table 5.

It can therefore be seen that the expected failure rate is extremely low for any reasonable operating temperature.

The analysis presented here was performed assuming Poisson statistics for the failure rate. From the high statistics, high temperature accelerated ageing tests performed by the manufacturer of the VCSELs used in this work, a good fit was obtained to a Weibull distribution [14]. The Weibull distribution for the failure times t is of the form

$$f(t) = \frac{\alpha}{\beta^{\alpha}}t^{\alpha-1}\exp(-t/\beta). \tag{1.4}$$

The parameter α can be regarded a measure of the deviation from an exponential (as expected for Poisson statistics) and in the case $\alpha = 1$, the Weibull function reduces to an exponential with a Mean Time To Failure (MTTF) equal to β. The fit of the manufacturer's accelerated ageing data gave a value of $\alpha = 1.7$ [14]. A Weibull function of the form of Eq (1.4) with this value of α was used to analyse the data obtained in this study (no failures in 20 devices, operated for 2534 h at 100°C). The resulting 90% c.l. upper limit on the MTTF is 8990 h, which is significantly less than the value of 22 000 h obtained with the assumption of Poisson statistics.

This MTTF can then be scaled with the acceleration factors from the Arrhenius equation and the expected failure rates for 10 years of ATLAS operation can be computed. The resulting predicted failure rates were much lower than those calculated assuming Poisson statistics (given in Table 5). This result is a general feature of the Weibull function which peaks at non-zero values of time, t, compared to the exponential distribution which always peaks at $t = 0$. Therefore weaker limits will be obtained on the MTTF for the Weibull distribution. However, the predicted failure rates for values of t much less than the

Table 5
Ninety per cent c.l. upper limits on VCSEL failure rates for 10 yr of ATLAS operation for different operating temperatures

Operating temperature (°C)	Failure rate (%)
0	3.7×10^{-4}
10	1.7×10^{-3}
20	6.8×10^{-3}
30	2.5×10^{-2}
40	8.5×10^{-2}
50	2.7×10^{-1}
60	7.9×10^{-1}

[12] Non-Return-to-Zero.

MTTF (as is the case for LHC operation) will be lower.

7. Conclusions

A sample of VCSEL was irradiated with 30 MeV protons to a fluence which was 40% higher than expected for the worst case in the SCT. This 30 MeV proton irradiation data for the VCSELs showed that there were significant threshold shifts and decreases in slope efficiency for the VCSELs. However, a lot of the radiation damage could be annealed by one week of operation at a constant current of 10 mA. After one further week of annealing at 20 mA nearly complete annealing of the threshold current and complete annealing of the slope efficiency were observed. During ATLAS operation, the VCSELs will be operated at a current of 10 mA whilst sending data, therefore a long period for annealing will occur. If necessary the VCSELs could be operated at a current of 20 mA during periods with no beam. The radiation damage data from 24 GeV protons showed similar behaviour as expected from the NIEL hypothesis. As expected for VCSELs, the gamma irradiation showed no significant degradation in VCSEL performance even for a dose of a factor of 6 higher than expected for the worst case in the SCT. From the accelerated ageing tests of the irradiated VCSELs, the expected failure rate for the 10 years of ATLAS operation is very low. Therefore these VCSELs can be considered qualified for reliable operation in the SCT.

Acknowledgements

We would like to thank the operators of the Mega Curie Irradiation plant and TR-30 Cyclotron Facility of INER, Taiwan, for help with the gamma and proton irradiation. This work was supported by the Atomic Energy Council and National Science Council of Taiwan, ROC. Financial support from the UK Particle Physics and Astronomy Research Council is gratefully acknowledged.

References

[1] ATLAS Inner Detector Technical Design Report, CERN/LHCC/97-16/17.
[2] D.G. Charlton, et al., Nucl. Instr. and Meth. A 443 (1999) 430.
[3] D.J. White, et al., Nucl. Instr. and Meth. A 457 (2001) 369.
[4] J.D. Dowell, et al., Nucl. Instr. and Meth. A 424 (1999) 483.
[5] D.G. Charlton, et al., Nucl. Instr. and Meth. A 456 (2001) 300.
[6] J. Beringer, et al., Nucl. Instr. and Meth. A 435 (1999) 375.
[7] D.G. Charlton, et al., Radiation tests of optical link components for the ATLAS SCT, Proceedings of the Fourth Workshop on Electronics for the LHC, Rome, 21–25 September 1998, CERN/LHCC/98-36.
[8] G. Mahout, et al., Nucl. Instr. and Meth. A446 (2000) 426.
[9] G. Mahout, et al., Proc. SPIE Photonics Space Environ. 4134 (2000) 214.
[10] I.M. Gregor, et al., In: Kent D. Choquette, Chun Lei (Eds.) Vertical-Cavity Surface-Emitting Lasers IV, Proc. SPIE 3946 (2000) 187–195.
[11] B. Hawthorne, Honeywell optoelectronics reliability study, 850 nm VCSEL products, available on http://www.honeywell.com/vcsel/
[12] MIL-STD-833B, Test methods and procedures for microelectronics.
[13] MITEL Semiconductor, J. Jonsson, J. Isaksson, Introduction to VCSELs, Second Workshop on Optical Readout Technologies for ATLAS, Oxford, January 1999.
[14] Kai-Feng Huang, VCSEL and PIN for Optical Links, Second workshop on optical readout technologies for ATLAS, Oxford, January 1999, available on http://www.truelight.com.tw/english/news/present.htm
[15] E.A. Burke, et al., IEEE Trans. Nucl. Sci. 34 (6) (1987) 1220.
[16] G.P. Summers, et al., IEEE Trans. Nucl. Sci. 40 (6) (1993) 1372.
[17] A. Chilingarov, et al., Radiation damage due to NIEL in GaAs particle detectors, ATLAS INDET-No-134, June 1996.
[18] Information on the PS is available on http://psdoc.web.cern.ch/PSdoc/acc/ps/psdoc.html
[19] M-L Chu, Optical package for SCT barrel front-end opto-link, ATLAS EDMS note ATL-IS-ES-0009. Available on http://edmsoraweb.cern.ch:8001/cedarnew/edmsatlas.home